IL-4 directly signals tissue-resident macrophages to proliferate beyond homeostatic levels controlled by CSF-1

Stephen J. Jenkins,[1,2] Dominik Ruckerl,[1] Graham D. Thomas,[1] James P. Hewitson,[1] Sheelagh Duncan,[1] Frank Brombacher,[4] Rick M. Maizels,[1] David A. Hume,[3] and Judith E. Allen[1]

[1]Institute of Immunology and Infection Research, School of Biological Sciences; and [2]Medical Research Council Centre for Inflammation Research and [3]The Roslin Institute and Royal (Dick) School of Veterinary Studies, College of Medicine and Veterinary Medicine; University of Edinburgh, Edinburgh EH8 9YL, Scotland, UK
[4]International Centre for Genetic Engineering and Biotechnology and University of Cape Town, 7925 Cape Town, South Africa

Macrophages (MΦs) colonize tissues during inflammation in two distinct ways: recruitment of monocyte precursors and proliferation of resident cells. We recently revealed a major role for IL-4 in the proliferative expansion of resident MΦs during a Th2-biased tissue nematode infection. We now show that proliferation of MΦs during intestinal as well as tissue nematode infection is restricted to sites of IL-4 production and requires MΦ-intrinsic IL-4R signaling. However, both IL-4Rα–dependent and –independent mechanisms contributed to MΦ proliferation during nematode infections. IL-4R–independent proliferation was controlled by a rise in local CSF-1 levels, but IL-4Rα expression conferred a competitive advantage with higher and more sustained proliferation and increased accumulation of IL-4Rα$^+$ compared with IL-4Rα$^-$ cells. Mechanistically, this occurred by conversion of IL-4Rα$^+$ MΦs from a CSF-1–dependent to –independent program of proliferation. Thus, IL-4 increases the relative density of tissue MΦs by overcoming the constraints mediated by the availability of CSF-1. Finally, although both elevated CSF1R and IL-4Rα signaling triggered proliferation above homeostatic levels, only CSF-1 led to the recruitment of monocytes and neutrophils. Thus, the IL-4 pathway of proliferation may have developed as an alternative to CSF-1 to increase resident MΦ numbers without coincident monocyte recruitment.

CORRESPONDENCE
Stephen J. Jenkins:
stephen.jenkins@ed.ac.uk

Abbreviations used: FSC, forward scatter; GI, gastrointestinal; *Hp*, *Heligmosomoides polygyrus bakeri*; *Ls*, *Litomosoides sigmodontis*; MΦ, macrophage; SSC, side scatter.

The number of resident macrophages (MΦs) in several tissues can apparently be maintained without replenishment from blood monocytes and other hematopoietic precursors (Volkman et al., 1983; Kanitakis et al., 2004; Ajami et al., 2007; Klein et al., 2007; Murphy et al., 2008; Schulz et al., 2012; Yona et al., 2013) through in situ proliferation (Chorro et al., 2009; Davies et al., 2011; Jenkins et al., 2011; Hashimoto et al., 2013). Local proliferation restores homeostatic numbers of resident lung and peritoneal MΦs after their loss as a result of acute inflammation (Davies et al., 2011; Hashimoto et al., 2013) but can act also as an inflammatory mechanism, leading to an outgrowth of tissue-resident MΦs beyond homeostatic levels. For example, infection with the rodent filarial nematode *Litomosoides sigmodontis* (*Ls*) causes a pleuritis characterized by expansion of the resident MΦ population to high densities equivalent to that reached by recruited monocyte-derived MΦs during classical inflammation (Jenkins et al., 2011). Similarly, Langerhans cells and microglia increase in density via elevated self-renewal during atopic dermatitis and experimental autoimmune encephalitis, respectively (Chorro et al., 2009; Ajami et al., 2011).

Proliferation, differentiation, and survival of MΦs are controlled by the CSF1R ligands CSF-1 and IL-34 produced by local tissue stroma to regulate the density of resident MΦs (Hume and MacDonald, 2012). CSF-1 administration to mice can increase blood monocyte and tissue MΦ numbers (Hume et al., 1988). Mice lacking

G.D. Thomas's present address is La Jolla Institute for Allergy and Immunology, La Jolla, CA 92037.

The Rockefeller University Press $30.00
J. Exp. Med. 2013 Vol. 210 No. 11 2477-2491
www.jem.org/cgi/doi/10.1084/jem.20121999

the CSF1R exhibit an extreme deficit in resident MΦs in many tissues (Dai et al., 2002), and the same cells are ablated in a time-dependent manner after treatment with a blocking anti-CSF1R antibody (MacDonald et al., 2010). A proliferative signal through the CSF1R has been shown to maintain homeostatic numbers of resident peritoneal MΦs in the steady-state (Davies et al., 2013) and mediate repopulation of resident lung and peritoneal MΦs after acute inflammation or experimental depletion (Davies et al., 2013; Hashimoto et al., 2013). CSF1R signaling can also control in vivo proliferation of monocyte-derived MΦs, required for the population of the growing myometrium in pregnancy (Tagliani et al., 2011) or maintenance of recruited cells during the resolution phase of sterile peritonitis (Davies et al., 2013).

The Th2 lymphokine IL-4 was first shown to regulate proliferation and accumulation of resident MΦs in the context of filarial nematode infection. Moreover, serial administration of an rIL-4 complex (IL-4c) was sufficient to induce proliferation and accumulation of MΦs throughout the body, including in the peritoneal cavity and liver (Jenkins et al., 2011), lung, and spleen (unpublished data), and to drive proliferation of recruited monocyte-derived cells (Jenkins et al., 2011). These studies did not reveal whether the actions of IL-4 were direct or indirect.

Akt signaling is required for CSF-1–mediated proliferation (Smith et al., 2000; Irvine et al., 2006; Huynh et al., 2012), and we have recently shown that intact Akt signaling is critically important for in situ MΦ proliferation in response to IL-4 (Rückerl et al., 2012). However, IL-4 receptor (IL-4R) signaling does not effectively activate Akt in MΦs in vitro despite phosphorylating PKB (Heller et al., 2008), thus raising the possibility that IL-4 acts via CSF1R signaling to induce Akt-dependent MΦ proliferation. Indeed, many important parallels exist between IL-4– and CSF-1–activated MΦs. For example, both IL-4 and CSF-1 promote a suppressive and a pro-repair phenotype in MΦs (Alikhan et al., 2011). Furthermore, the transcription factors c-Myc and KLF-4 are critical for both the "alternative activation" state induced in MΦs by engagement of the IL-4R (Liao et al., 2011; Pello et al., 2012) and CSF-1–dependent proliferation that occurs in the absence of Maf B and c-Maf (Aziz et al., 2009). Thus, understanding the relationship between CSF-1 and IL-4 is important, not least because several groups have used CSF-1 to generate human "M2" MΦs (Verreck et al., 2004; Martinez et al., 2006; Fleetwood et al., 2007), which are often considered highly parallel to alternatively activated MΦs driven by IL-4.

This study seeks to determine the contribution of CSF-1 to IL-4–driven MΦ proliferation and alternative activation. Alternatively activated MΦs are a distinguishing feature of inflammation driven by helminth infections and allergy but may also appear in cold-stressed adipose tissue (Nguyen et al., 2011; Karp and Murray, 2012), certain immunogenic tumors (DeNardo et al., 2009; Linde et al., 2012), and even the steady-state (Wu et al., 2011). Using direct delivery of IL-4 and Th2-biased infection models, we demonstrate that IL-4–mediated proliferation requires MΦ-intrinsic IL-4Rα signaling that is entirely independent of the CSF1R. However, these experiments revealed a significant contribution of IL-4Rα–independent, CSF1R-dependent MΦ proliferation during nematode infection. We further demonstrate that IL-4Rα expression confers a major competitive advantage to MΦs, such that IL-4Rα$^+$ cells rapidly outcompete those lacking receptor expression.

RESULTS

IL-4–dependent proliferation does not require the CSF1R

We used delivery of IL-4c as a reductionist approach to investigate whether IL-4 acts via the CSF1R to drive expansion of resident serous cavity MΦs. Ki67 expression was used to determine the frequency of all F4/80^{High} MΦs in cycle, as described previously (Jenkins et al., 2011), whereas a 3-h BrdU pulse before necropsy or high level of Ki67 expression (Ki67^{High}) was used to identify cells in S phase (Fig. S1 A; Landberg et al., 1990). Intracellular staining for RELMα and/or Ym1 was used as a marker of alternative activation. Consistent with the established role of CSF-1 in regulating steady-state MΦ levels (Davies et al., 2013), proliferation observed in control PBS-treated mice was completely blocked by treatment with anti-CSF1R mAb (Fig. 1 A). In contrast, neither elevated proliferation nor marker induction by IL-4c was affected by antibody treatment (Fig. 1 A). The only influence of blocking CSF1R on IL-4c treatment was to reduce the final MΦ number (Fig. 1 A). Daily oral gavage of GW2580, an inhibitor of the CSF1R tyrosine kinase, also had no effect on IL-4–induced MΦ proliferation or alternative activation (Fig. 1 B). Furthermore, *Csf1r* gene expression was significantly reduced in FACS-purified peritoneal MΦs 24 h after injection of IL-4c (Fig. 1 C). As expected, because the ligand is cleared by receptor-mediated endocytosis (Hume and MacDonald, 2012), CSF1R blockade resulted in elevated levels of CSF-1 in the tissue and bloodstream (Fig. 1 D), thereby confirming the effectiveness of the antibody. However, CSF-1 production was not increased in response to IL-4 (Fig. 1 D). Thus, in the context of IL-4 delivery, there was no evidence of CSF1R involvement in proliferation and alternative activation.

IL-4–driven proliferation requires MΦ-intrinsic IL-4Rα signaling

We next addressed the possibility that IL-4 signals directly to MΦs to induce proliferation. We used *LysM^{cre}Il4ra$^{-/lox}$* mice to delete the IL-4Rα chain on myeloid cells including MΦs and neutrophils (Herbert et al., 2004). Injection of IL-4c into *LysM^{cre}Il4ra$^{-/lox}$* mice resulted in elevated proliferation of F4/80^{High} MΦs in the cavities as well as elevated frequencies of alternatively activated MΦs (Fig. 2 A). Nevertheless, MΦ proliferation was lower in *LysM^{cre}Il4ra$^{-/lox}$* mice than in *Il4ra$^{-/lox}$* controls (pleural, $P < 0.01$; peritoneal, $P < 0.001$; Fig. 2 B). Co-staining for RELMα and BrdU (Fig. 2 B) revealed that RELMα$^+$ MΦs from *LysM^{cre}Il4ra$^{-/lox}$* mice underwent significantly greater levels of proliferation than RELMα$^-$ cells. Because RELMα expression is a known marker of IL-4Rα engagement on MΦs (Jenkins and Allen, 2010) and LysM-Cre is relatively inefficient (Hume, 2011), the data

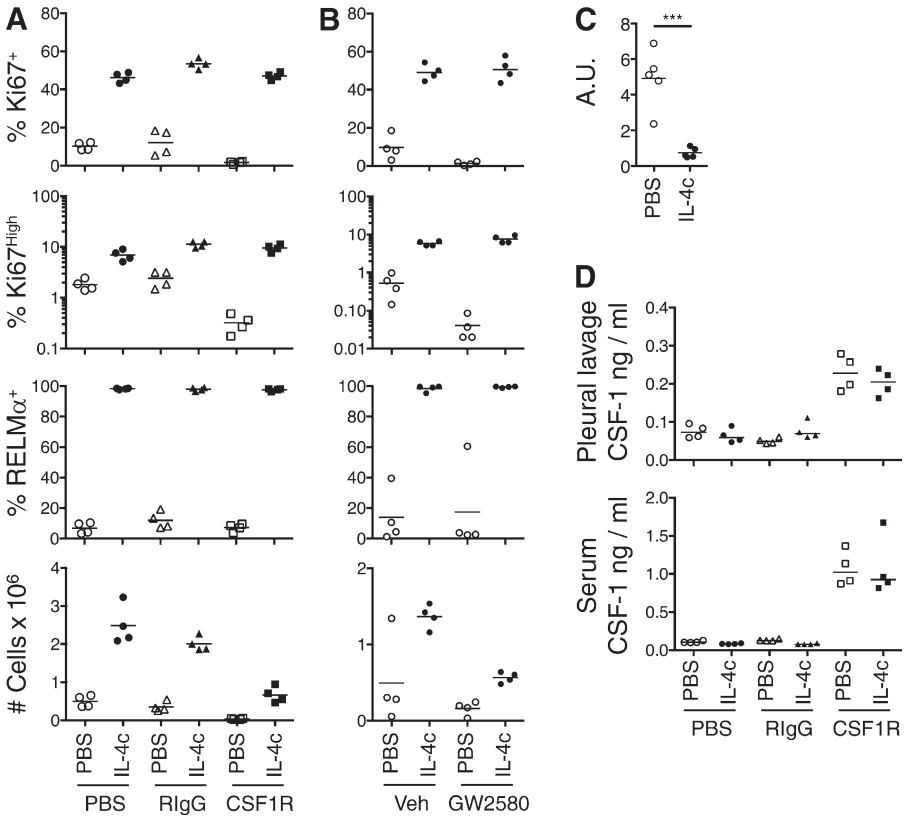

Figure 1. IL-4 drives CSF-1–independent MΦ proliferation. (A) BL/6 mice were injected i.p. with IL-4c or PBS plus anti-CSF1R mAb (CSF1R), rat IgG (RIgG), or PBS on days 0 and 2. The proportion of F4/80^{High} pleural MΦs positive for Ki67, Ki67^{High}, or RELMα and total MΦ numbers were determined by flow cytometry on day 2 after the last injection. Graphs depict individual data for four mice/group. (B) As in A, but on day 3 after daily oral gavage with vehicle control or GW2580 on days 0–3. (C) Mice were injected with a single dose of PBS or IL-4c, and the expression of CSF1R mRNA was determined 24 h later in FACS-purified F4/80^{High} peritoneal MΦs. ***, $P < 0.001$ determined by two-tailed Student's *t* test. Individual data for five mice/group are shown. (D) CSF-1 levels in pleural lavage fluid and serum from mice in A determined by ELISA. All data are representative of two to three separate experiments, with the same results observed in the peritoneal cavity. (A–D) Horizontal bars indicate mean values.

suggest that IL-4–dependent proliferation predominantly occurs in the subset of MΦs that retain the IL-4R in *LysM^{cre} Il4ra$^{-/lox}$* animals.

To confirm this conclusion, *Il4ra$^{+/+}$Cd45.1^{+}Cd45.2^{+}* C57BL/6 mice were lethally irradiated and transplanted with a 50:50 mix of BM from *Il4ra$^{+/+}$Cd45.1^{+}Cd45.2^{+}* and *Il4ra$^{-/-}$ Cd45.2$^{+/+}$Cd45.1^{null}* mice, so that cells derived from *Il4ra$^{-/-}$* BM could be distinguished from WT by a lack of CD45.1 expression. Blood-borne monocytes (Fig. 2 C) and other myeloid populations (not depicted) exhibited roughly equal proportions of CD45.1^{+} and CD45.1^{-} cells 8 wk after reconstitution. This extends earlier data showing the key mediator of IL-4R signaling, STAT6, has no intrinsic role in steady-state proliferation or survival of hematopoietic stem cells despite their ubiquitous IL-4Rα^{+} expression (Bunting et al., 2004). Likewise, similar frequencies of *Il4ra$^{+/+}$* and *Il4ra$^{-/-}$* cells were detected in the resident F4/80^{High} pleural and peritoneal cavity MΦ populations in control mice treated with PBS (Fig. 2 D and not depicted). In contrast, *Il4ra$^{+/+}$* F4/80^{High} MΦs greatly outnumbered *Il4ra$^{-/-}$* cells in the pleural and peritoneal cavities of mice treated with IL-4c. Indeed, only the IL-4Rα^{+} population increased in number after treatment with IL-4c (Fig. 2 D and not depicted), consistent with increased S-phase BrdU^{+} cells (Fig. 2 E) and Ki67^{+} cells (not depicted) being observed only in the CD45.1^{+} IL-4Rα^{+} cells. Notably, steady-state levels of proliferation in PBS-treated controls did not differ between *Il4ra$^{+/+}$* and *Il4ra$^{-/-}$* cells, suggesting IL-4 is only important in an inflammatory context. Intracellular staining for RELMα (not depicted) and Ym1 (Fig. 2 E) in these experiments confirmed an absolute requirement for intrinsic IL-4Rα signaling to up-regulate production of these archetypal alternative activation markers under this reductionist condition.

Both IL-4Rα–dependent and –independent pathways contribute to proliferation during nematode infection

The Th2 cytokines IL-4 and IL-13 can both signal via the IL-4Rα to drive alternative activation (Gordon and Martinez, 2010). In our previous study, nematode-associated increased MΦ proliferation was not entirely absent in *Il4$^{-/-}$* mice (Jenkins et al., 2011), suggesting a possible contribution from IL-13. To assess the potential of IL-13 to induce proliferation, mice were injected with IL-13 complexed with a neutralizing antibody (IL-13c). IL-13c led to significant ($P < 0.01$) MΦ proliferation, at a similar magnitude to IL-4c delivery (Fig. 3 A), but as documented previously (Heller et al., 2008), IL-13 was somewhat less effective at stimulating RELMα production by MΦs. To determine whether IL-13 was responsible for the residual rise in proliferation observed in nematode-infected *Il4$^{-/-}$* mice, we infected mice lacking the IL-4Rα chain (*Il4ra$^{-/-}$*). Proliferation and accumulation of pleural MΦs after *Ls* infection were significantly ($P < 0.001$) reduced in *Il4ra$^{-/-}$* mice compared with WT controls (Fig. 3 B) but to no greater extent than in the *Il4$^{-/-}$* mice (Jenkins et al., 2011), suggesting no contribution of IL-13. In contrast, marker induction in MΦs was entirely dependent on IL-4Rα signaling

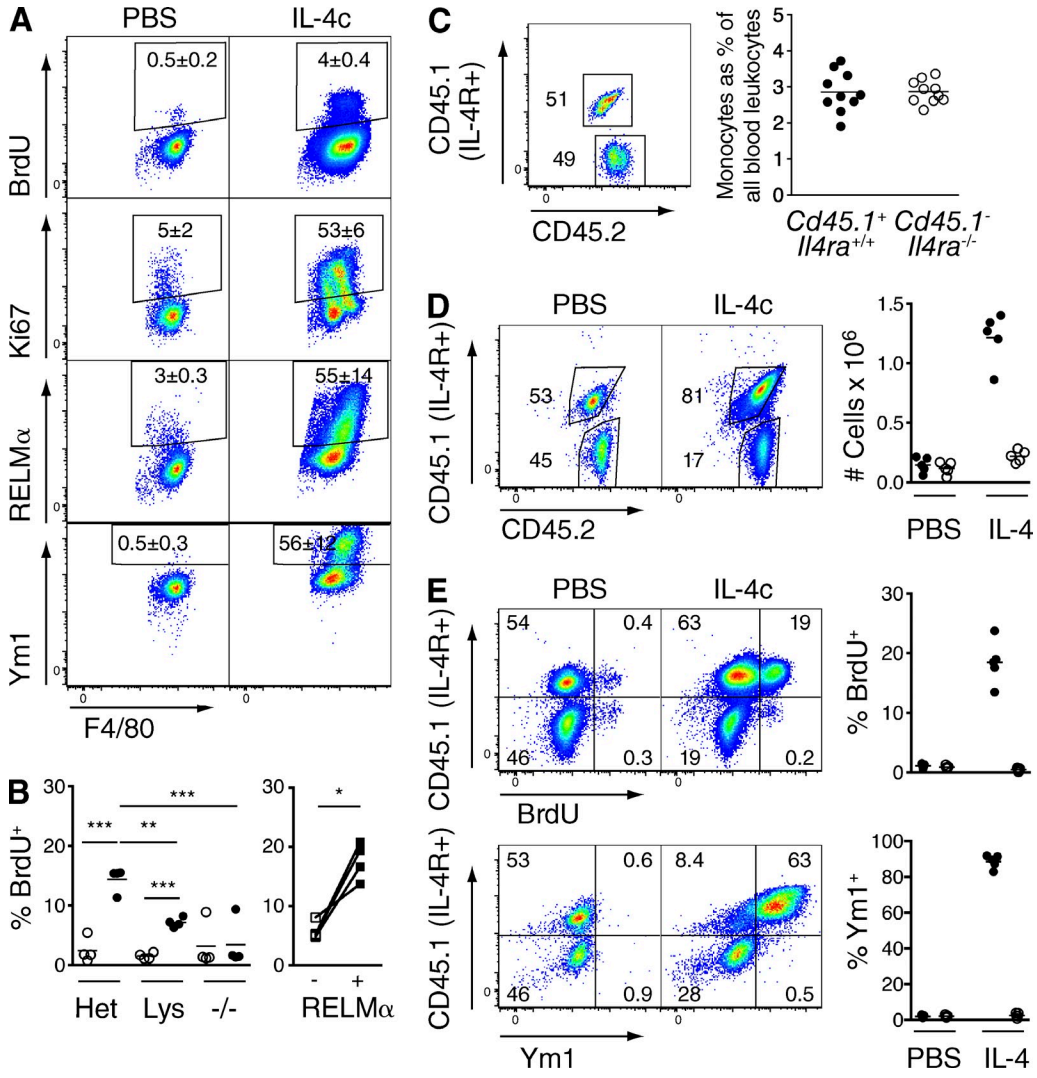

Figure 2. MΦ-intrinsic IL-4Rα signaling is essential for proliferation and alternative activation triggered by IL-4c. (A) *LysM*^{cre}*Il4ra*$^{-/lox}$ BALB/c mice were injected i.p. on days 0 and 2 with PBS or IL-4c, and peritoneal lavage cells were analyzed on day 4 by flow cytometry for BrdU incorporation or Ki67, RELMα, and Ym1 versus F4/80 expression. Representative flow cytograms gated on F4/80^{High} peritoneal MΦs with frequencies depicting the mean ± SEM of four mice per group. (B) *Il4ra*$^{-/lox}$ (Het), *LysM*^{cre}*Il4ra*$^{-/lox}$ (Lys), or *Il4ra*$^{-/-}$ (−/−) BALB/c were treated with PBS (open) or IL-4c (closed) as in A, and BrdU incorporation by F4/80^{High} pleural MΦs was determined on day 3 together with the frequency of BrdU^{+} cells in RELMα-positive (+) or negative (−) F4/80^{High} MΦs from the IL-4c–treated *LysM*^{cre}*Il4ra*$^{-/lox}$ group. *, $P < 0.05$; **, $P < 0.01$; and ***, $P < 0.001$ determined by ANOVA (left) or paired Student's *t* test (right). Data are representative of four independent experiments inclusive of data in A, with three to four mice/group. (C) BL/6 *Il4ra*$^{+/+}$*Cd45.1*$^{+}$*Cd45.2*$^{+}$ mice were lethally irradiated and reconstituted with a 50:50 mix of *Il4ra*$^{+/+}$*Cd45.1*$^{+}$*Cd45.2*$^{+}$ and *Il4ra*$^{-/-}$*Cd45.1*^{null}*Cd45.2*$^{+/+}$ congenic BM cells. The frequency of blood monocytes (gated as side scatter [SSC]^{low}CD11b^{+}CD115^{+}) derived from each BM was determined by analysis of CD45.1 and CD45.2 expression 8 wk later. A representative flow cytogram of CD45.1 and CD45.2 expression on blood monocytes is shown together with a graph depicting the frequency of CD45.1^{+} and CD45.1^{-} monocytes in all blood leukocytes from 10 individual mice. (D) Mice from C were subsequently injected i.p. twice, 2 d apart, with PBS or IL-4c, and pleural lavage cells were analyzed 2 d after the last injection for CD45.1 and CD45.2 expression. Representative flow cytograms gated on all live F4/80^{High} MΦs are shown together with a graph depicting the total number of *Il4ra*$^{+/+}$*Cd45.1*$^{+}$ (closed circles) and *Il4ra*$^{-/-}$*Cd45.1*^{null} (open circles) pleural F4/80^{High} MΦs in each group, with individual data for five mice/group presented. (E) Representative flow cytograms depicting CD45.1 expression versus BrdU incorporation or Ym1 expression gated on single F4/80^{High}CD19^{-} pleural MΦs from mice in D, and graphs showing the proportion of *Il4ra*$^{+/+}$*Cd45.1*$^{+}$ (closed circles) and *Il4ra*$^{-/-}$*Cd45.1*^{null} (open circles) F4/80^{High}CD19^{-} MΦs positive for BrdU or Ym1 for individual mice. (C–E) Data are representative of two experiments. (B–E) Horizontal bars indicate mean values.

(Fig. 3 B), and worm burdens did not significantly differ between strains at this stage of infection (not depicted). Hence, mechanisms independent of IL-4Rα contribute to elevated MΦ self-renewal during nematode infection. Comparison of the kinetics of alternative activation and proliferation stimulated by IL-4c versus *Ls* infection revealed key differences: IL-4c induced marker expression in peritoneal and pleural MΦs before detectable proliferation (Fig. 3 C and Fig. S1 B), whereas during infection proliferation preceded marker expression (Fig. 3 D). The data indicate that IL-4Rα–independent

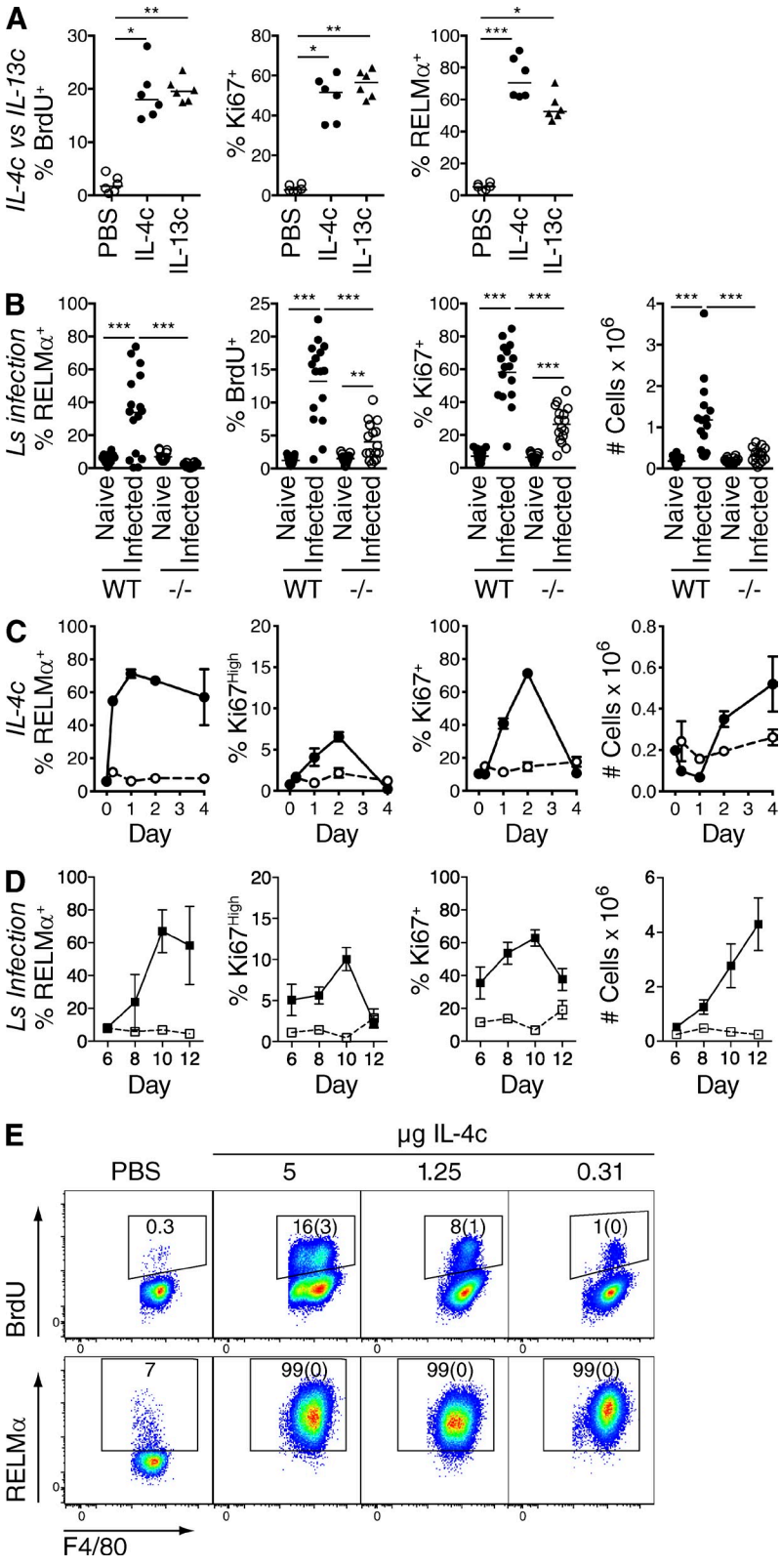

Figure 3. IL-4Rα–dependent and –independent mechanisms of proliferation during nematode infection. (A) BL/6 mice were given a single i.p. injection of IL-13c, IL-4c, or PBS, and the proportion of BrdU$^+$, Ki67$^+$, and RELMα$^+$ F4/80^{High} peritoneal MΦs was determined 36 h later. Graphs depict individual data for six mice per group and are representative of two independent experiments. Horizontal bars indicate median values. Equivalent results were obtained in the pleural cavity. *, $P < 0.05$; **, $P < 0.01$; and ***, $P < 0.001$ determined by Kruskal-Wallis test. (B) C57BL/6 (WT) and *Il4ra*$^{-/-}$ (−/−) mice were infected with *Ls*, and the total number of F4/80^{High} pleural MΦs and the proportion positive for BrdU, Ki67, and RELMα were determined on day 10. Results are pooled from two experiments with 15–16 mice/group shown. Horizontal bars indicate mean values. **, $P < 0.01$; and ***, $P < 0.001$ determined by ANOVA. (C) BL/6 mice were given a single i.p. dose of IL-4c (solid line) or PBS (dashed line), after which the total number of pleural cavity F4/80^{High} MΦs and the proportion positive for RELMα, Ki67^{High}, or Ki67 were determined over a 4-d time course. Data are mean ± SEM of four mice/group and representative of two experiments, with the same results obtained for peritoneal MΦs. Day 0 represents naive. (D) As C but from *Ls*-infected (solid line) or naive (dashed line) mice. Data are mean ± SEM from four to five mice per group and representative of three experiments. (E) Representative flow cytograms of F4/80^{High} peritoneal MΦs 4 d after i.p. injection of PBS or IL-4c containing 5, 1.25, or 0.31 μg IL-4 on days 0 and 2. Frequencies are means with SEM in parentheses of three to six IL-4c–treated animals per group or a single value for pooled cells from three PBS-treated mice. A repeat using a single injection regimen verified dose effect for both of IL-4c and IL-13c.

proliferation occurs early during infection with subsequent peak proliferation driven by IL-4.

Of note, proliferation induced by a single IL-4c dose subsided after 4 d, whereas alternative activation markers were sustained (Fig. 3 C and Fig. S1 B). After two sequential IL-4c doses at days 0 and 2, proliferation remained evident at day 4 (Fig. 1 A). We therefore titrated the dose of IL-4c. As expected, proliferative activity required high doses of IL-4,

whereas induction of RELMα was maximal at the lowest dose tested (Fig. 3 E). Thus, detection of alternative activation markers in the tissues is not synonymous with proliferation, as marker expression may only indicate prior or low-level exposure to IL-4.

IL-4 switches MΦs to CSF-1–independent proliferation

We used CSF1R blockade to assess the potential contribution of CSF1R signaling to the IL-4Rα–independent proliferation that occurs during *Ls* infection. Mice were treated with anti-CSF1R mAb between days 8 and 10 to coincide with the approximate onset of alternative activation (Fig. 3 D) and when IL-4R–independent proliferation is detectable (Fig. 3 B). CSF1R blockade led to a significant reduction in infection-induced proliferation of pleural MΦs (Fig. 4 A), whereas alternative activation (Fig. 4 A), Th2 responses, and worm burden (not depicted) were unaffected. However, the response in the infected group appeared bimodal, with 13 of 20 anti-CSF1R–treated mice showing almost complete inhibition of proliferation (Fig. 4 A, black squares), whereas the remaining animals were similar to controls (Fig. 4 A, gray squares). The anti-CSF1R–treated infected animals in which high-level proliferation remained evident showed the highest frequencies of $Ym1^+$ MΦs (Fig. 4 A, gray squares), and indeed the frequency of MΦs able to proliferate in the presence of anti-CSF1R correlated positively with $Ym1^+$ MΦs (Spearman $r = 0.84$, $P < 0.0001$). The data suggest that as the strength of Th2 response and corresponding IL-4Rα signaling increased, the dependence on CSF1R signaling for MΦs to proliferate and accumulate during tissue nematode infection declined. In other words, IL-4 can substitute for CSF-1.

CSF-1 is increased in the circulation and local lesions in many infections, chronic inflammation, and malignancy (Chitu and Stanley, 2006; Hume and MacDonald, 2012). We therefore measured levels of cytokine in the pleural lavage fluid and serum. There was a modest increase in accumulation of CSF-1 in the pleural cavity of infected anti-CSF1R–treated mice compared with naive controls, but no increase in the serum (Fig. 4 B). No correlation was found between the level of pleural CSF-1 and frequency of $BrdU^+$ MΦs in anti-CSF1R–treated infected mice (Spearman $r = 0.1398$, $P = 0.5565$), consistent with IL-4R signaling controlling CSF-1–independent proliferation in these mice directly rather than via elevation of CSF-1.

IL-4Rα expression provides a competitive advantage to MΦs during nematode infection

We next infected $Il4ra^{+/+}Cd45.1^+$: $Il4ra^{-/-}Cd45.1^{null}$ mixed BM chimeric mice with *Ls* to investigate the relevance of MΦ-intrinsic IL-4Rα signaling in a setting in which IL-4Rα–independent proliferation can occur. In contrast to the highly restricted response seen in these mice after IL-4c injection (Fig. 2, D and E), increased proliferation of both $Il4ra^{+/+}$ and $Il4ra^{-/-}$ pleural $F4/80^{High}$ MΦs was evident by day 10 after *Ls* infection (Fig. 5 A). However, the frequency of cycling cells was significantly greater in the IL-4Rα$^+$ population in all infected

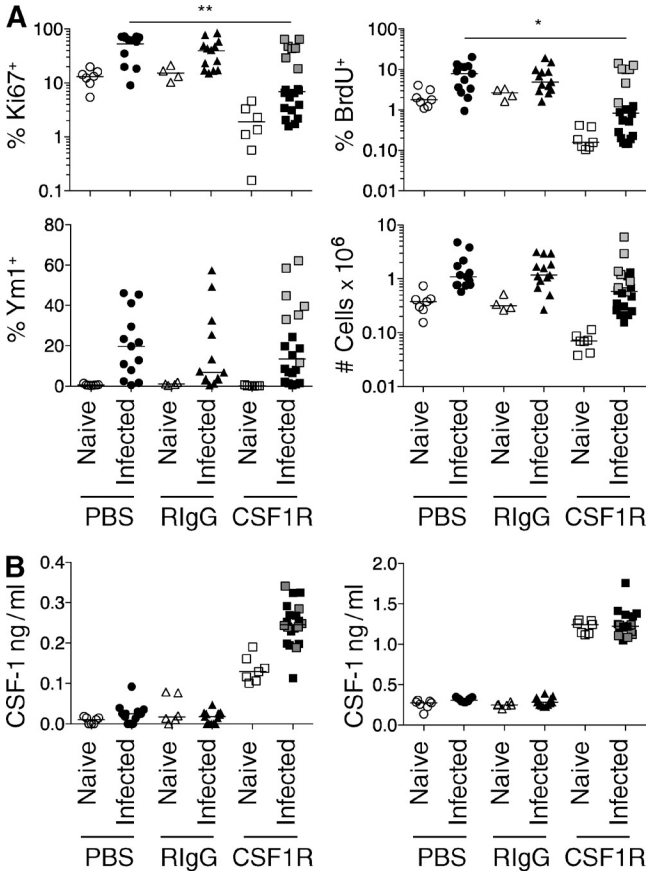

Figure 4. Elevated CSF-1 production contributes to MΦ proliferation during tissue nematode infection. (A) BL/6 mice were infected with *Ls* and injected i.p. on day 8 with anti-CSF1R mAb (CSF1R), rat IgG (RIgG), or PBS. Total number of $F4/80^{High}$ pleural MΦs and the proportion positive for BrdU, Ki67, or Ym1 were determined on day 10. Data are pooled from two experiments with 7, 13, and 20 mice for naive and PBS-, RIgG-, and anti-CSF1R–treated infected, groups, respectively. *, $P < 0.05$; and **, $P < 0.01$ determined by Kruskal-Wallis test. (B) CSF-1 levels in pleural lavage (left) or serum (right) from mice in A determined by ELISA. (A and B) Horizontal bars indicate median.

mice at this time ($P < 0.001$), and only in these cells did heightened proliferation remain evident at day 16 (Fig. 5 A). In contrast, production of Ym1 (Fig. 5 A) and RELMα (not depicted) during infection was wholly dependent on MΦ-intrinsic IL-4Rα signaling. Consistent with the pattern of proliferation, both $Il4ra^{+/+}$ and $Il4ra^{-/-}$ populations significantly increased in number in the pleural cavity by day 10 after infection ($P < 0.01$), yet by day 16 the IL-4Rα$^-$ MΦs, although still elevated in number ($P < 0.05$), were significantly outnumbered by the IL-4Rα$^+$ cells (Fig. 5 B; $P < 0.05$). The selective advantage provided by the IL-4Rα was only observed in the $F4/80^{High}$ MΦ population and not in other myeloid cells (Fig. 5 C). Thus, although confirming the existence of an IL-4Rα–independent pathway of proliferation, these data show that direct IL-4Rα signaling to MΦs conveys a competitive advantage during infection at least in part by enhancing entry into cell cycle. These findings explain the emergence of

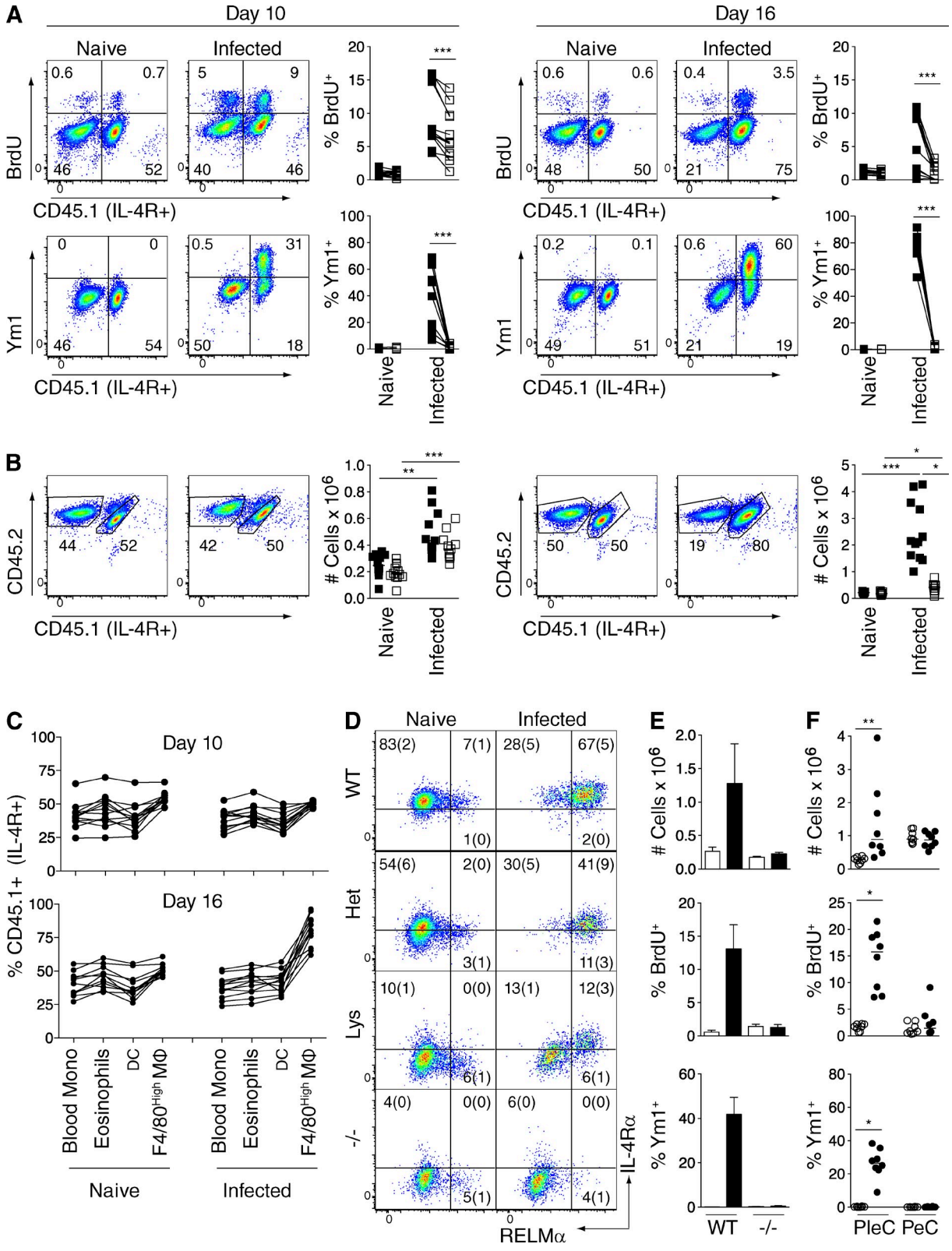

Figure 5. IL-4Rα signaling to MΦs provides a competitive advantage during tissue nematode infection. (A) BL/6 *Il4ra*$^{+/+}$*Cd45.1*$^{+}$*Cd45.2*$^{+}$ mice were lethally irradiated and reconstituted with a 50:50 mix of *Il4ra*$^{+/+}$*Cd45.1*$^{+}$*Cd45.2*$^{+}$ and *Il4ra*$^{-/-}$ *Cd45.1*^{null}*Cd45.2*$^{+/+}$ congenic BM cells over 8 wk. Mice were infected with *Ls*, after which BrdU incorporation or Ym1 expression versus expression of CD45.1 was determined on single F4/80^{High}CD19^{-} pleural MΦs at days 10 and 16 after infection. Representative flow cytograms are shown, whereas graphs depict the proportion of IL-4Rα^{+}CD45.1^{+} (closed

RELMα$^+$ pleural MΦs in MΦ-specific IL-4Rα–deficient *LysM^{cre}Il4ra$^{-/lox}$* mice during the later phase of *Ls* infection (Fig. 5 D). Indeed, by day 60 after infection, RELMα and YM1 expression by MΦs is indistinguishable between WT and *LysM^{cre}Il4ra$^{-/lox}$* mice (not depicted). IL-4Rα expression on MΦs in the *LysM^{cre}Il4ra$^{-/lox}$* mice was confirmed by surface staining (Fig. 5 D). Thus, IL-4Rα expression can give MΦs a competitive advantage during a chronic Th2 inflammatory setting such as helminth infection.

Proliferation during infection requires adaptive immunity and is localized to the infection site

We have previously established using *Rag1$^{-/-}$* mice that IL-4–driven MΦ proliferation per se does not require adaptive immunity (Jenkins et al., 2011). In the context of chronic nematode infection, however, MΦ accumulation requires Th2 cells and MHC class II (Loke et al., 2007). We thus assessed the requirement for adaptive immunity in MΦ proliferation during infection. There was a dramatic reduction in the number of F4/80$^+$ MΦs in nematode-infected *Rag1$^{-/-}$* mice compared with WT controls, matched by a complete failure of the MΦs to divide or up-regulate alternative activation markers (Fig. 5 E). Consistent with a need for cognate antigen-specific interaction, proliferation and alternative activation were localized to the site of parasite infection in WT animals, with significantly ($P < 0.05$) elevated responses observed in the pleural but not the peritoneal cavity of infected mice (Fig. 5 F).

IL-4–dependent MΦ proliferation, alternative activation, and competitive advantage are features of intestinal nematode infection

Oral infection of BALB/c mice with the gastrointestinal (GI) nematode *Heligmosomoides polygyrus bakeri* (*Hp*) leads to invasion of the submucosa of the duodenum where the worms undergo developmental maturation. Despite restriction of the worms to the GI tract, there is systemic dissemination of Th2 cells with selectivity for the peritoneal cavity (Mohrs et al., 2005). In *Hp*-infected mice, there was a striking increase in proliferation of F4/80^{High} resident MΦs by day 7 after infection in the peritoneal (Fig. 6 A) but not the pleural cavity (not depicted), consistent with the localized MΦ proliferation observed in our *Ls* model. Infection led to a two- to threefold increase in cells in the peritoneal lavage, exclusively within the F4/80^{High} MΦ population. As expected for a Th2 setting, these MΦs expressed RELMα and Ym1 (Fig. 6 A). As in the *Ls* model, *Il4$^{-/-}$* mice had a reduced response, although a significant increase in BrdU$^+$ ($P < 0.001$), Ki67$^+$ ($P < 0.001$), and total MΦs ($P < 0.01$) remained (Fig. 6 B). A minor population of Ym1$^+$ MΦs was also detected in infected *Il4$^{-/-}$* mice, suggesting a limited influence of IL-13 (Fig. 6 B). Blockade of CSF1R signaling demonstrated a CSF1R-dependent component to the proliferative but not the alternative activation response (Fig. 6 C), and thus as in the *Ls* model, both CSF1R and IL-4Rα signaling also contribute to MΦ proliferation in this model. We also reexamined the relative importance of cell-autonomous IL-4R signaling in the *Hp* model. The majority of F4/80^{High} MΦs, but not other myeloid cell populations, were IL-4Rα$^+$ by day 14 after infection of *Il4ra$^{+/+}$Cd45.1$^+$*: *Il4ra$^{-/-}$Cd45.1^{null}* mixed BM chimeric mice, despite earlier accumulation of both IL-4Rα$^+$ and IL-4Rα$^-$ cells (Fig. 6 D). This competitive advantage was confirmed using *LysM^{cre}Il4ra$^{-/lox}$* mice infected with *Hp*, in which the proportion of RELMα-positive cells increased from 4% in naive mice (not depicted) to 25% at day 14 and 70% by day 28 (Fig. 6 E), by which point >50% of the MΦs expressed IL-4Rα detectable by flow cytometry (not depicted). Infection with a GI nematode thus led to a MΦ response in the peritoneal cavity that mirrored the pleural cavity during infection with the filarial worm *Ls*. In both models, CSF1R and IL-4Rα contributed independently to proliferation.

Differing consequences of CSF-1– versus IL-4–induced inflammation

Because both IL-4 and CSF-1 can induce local MΦ proliferation, we sought to compare the MΦs elicited by the two stimuli. To assess the contribution of CSF-1 to cellular dynamics in the serous cavity, we used a new reagent, Fc–CSF-1 designed for stable in vivo delivery of CSF-1. We compared Fc–CSF-1 with IL-4c at similar molar doses that induced maximal levels of proliferation with both reagents (≥80% Ki67$^+$ by 48 h; not depicted). Despite near identical levels of MΦ proliferation at 24 h, only IL-4c induced RELMα (Fig. 7 A) or Ym1 (not depicted) production. Furthermore, Fc–CSF-1

squares) and IL-4Rα$^-$CD45.1$^-$ (open squares) cells positive for BrdU or Ym1, with each line illustrating paired measurements from individual mice. Data are pooled from two experiments, with 11–12 mice/group. ***, $P < 0.001$ determined by paired Student's *t* test. (B) CD45.1 and CD45.2 expression gated on all F4/80^{High} pleural MΦs from mice in A and graphical presentation of the total number of IL-4Rα$^+$CD45.1$^+$ (closed squares) and IL-4Rα$^-$CD45.2$^{+/+}$ (open squares) subsets of these cells. *, $P < 0.05$; **, $P < 0.01$; and ***, $P < 0.001$ determined by Kruskal-Wallis test. (C) Frequency of IL-4Rα$^+$CD45.1$^+$ cells within CD115$^+$CD11b$^+$SSC^{Low} blood monocytes and pleural cavity eosinophils (SSC^{High}, F4/80^{Low}, MHCII$^-$), DCs (CD11c^{High}MHCII^{High}), and F4/80^{High} MΦs at days 10 and 16 after infection of mice in A, with lines joining cells of individual mice. (D) *Il4ra$^{+/+}$* (WT), *Il4ra$^{-/lox}$* (Het), *LysM^{cre}Il4ra$^{-/lox}$* (Lys), or *Il4ra$^{-/-}$* (−/−) mice were infected with *Ls* or left naive, and RELMα and IL-4Rα staining on F4/80^{High} pleural MΦs was determined at day 17. Frequencies are means with SEM in parentheses of five to seven mice/group. The emergence of RELMα$^+$ MΦs in *LysM^{cre}Il4ra$^{-/lox}$* mice was confirmed in a further three independent experiments between days 14 and 60 after infection. (E) C57BL/6 (WT) or *Rag1$^{-/-}$* (−/−) mice were infected with *Ls*, and the total number of pleural cavity F4/80^{High} MΦs and the proportion incorporating BrdU or expressing Ym1 were determined on day 10, with mean and SEM of five mice/group shown. (F) As in E, but both peritoneal (PeC) and pleural (PleC) cavity F4/80^{High} MΦs from naive (open circles) or *Ls*-infected C57BL/6 mice were analyzed at 10 d after infection. Data are representative of three experiments with eight mice/group. *, $P < 0.05$; and **, $P < 0.01$ determined by Kruskal-Wallis test. (B and F) Horizontal bars indicate median values.

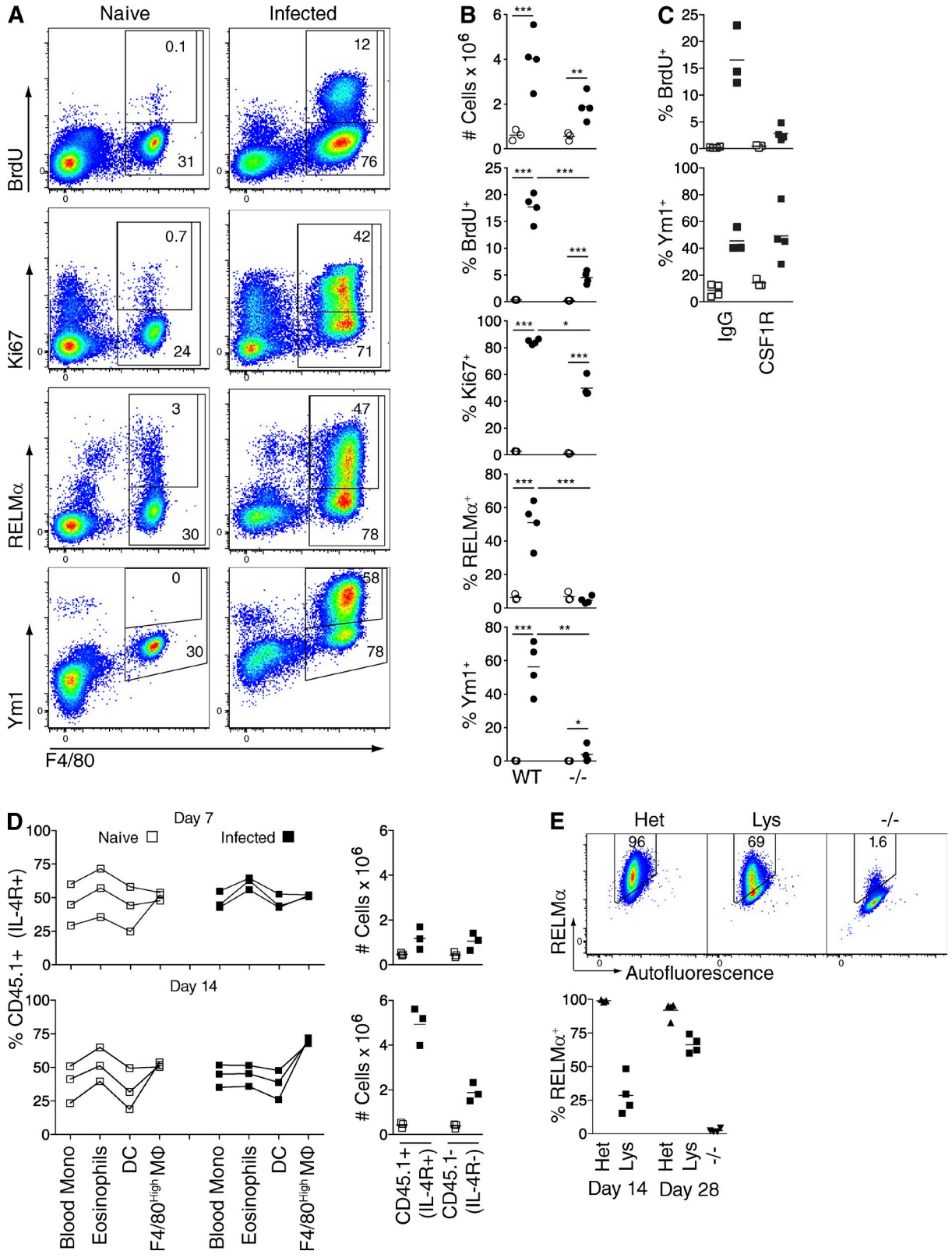

Figure 6. IL-4–dependent proliferation occurs during GI nematode infection and provides a competitive advantage to IL-4Rα⁺ MΦs. (A) BALB/c mice were infected orally with *Hp*, and peritoneal lavage cells were assessed at day 7. Representative flow cytograms of all peritoneal cells showing gates and frequencies for all or BrdU⁺, Ki67⁺, RELMα⁺ or Ym1⁺, F4/80^{High} MΦs. Data are representative of five experiments. (B) BALB/c (WT) or *Il4*$^{-/-}$ (−/−) mice were infected with *Hp* (closed symbols) or left naive (open symbols), and the total peritoneal F4/80^{High} MΦs and the proportion

induced the recruitment of inflammatory cells including neutrophils and Ly-6C$^+$ monocytes (Fig. 7 B), consistent with its recently described ability to drive proinflammatory chemokine production (Tagliani et al., 2011) and acute monocytopenia (Ulich et al., 1990). In striking contrast, no inflammatory recruitment was seen with IL-4c, consistent with the ability of IL-4 to actively down-regulate proinflammatory chemokines (Thomas et al., 2012). Thus although CSF-1 and IL-4 both induce MΦ proliferation in the tissues, they have otherwise markedly different consequences. Additionally, these data demonstrate that elevated CSF-1 signaling is sufficient to stimulate heightened proliferation (Fig. 7 A) and accumulation (not depicted) of resident MΦs in vivo without need for additional signals that occur during infection/inflammation and provide some explanation for the elevated peritoneal MΦ numbers seen in the original study of systemic CSF-1 treatment of mice (Hume et al., 1988).

DISCUSSION

We previously demonstrated the requirement for IL-4 to achieve maximal proliferation of MΦs during nematode infection and an absolute requirement for IL-4Rα for MΦ proliferation after IL-4c delivery (Jenkins et al., 2011). Our working hypothesis was that IL-4 acted indirectly via an intermediate cell, to stimulate production of a MΦ mitogenic factor, such as CSF-1, similar to the process by which a vitamin D3 analogue acts on keratinocytes to stimulate Langerhans cell proliferation (Chorro et al., 2009). This hypothesis was supported by our preliminary data in which IL-4–driven proliferation was observed in mice apparently lacking IL-4Rα on MΦs. However, using mixed BM chimeric mice, we demonstrate that MΦ-intrinsic IL-4Rα signaling is required for MΦ proliferation in response to endogenous or exogenous IL-4. Furthermore, IL-4–mediated proliferation was entirely independent of CSF1R signaling, in contrast to the homeostatic proliferation of cavity-resident MΦs, which is completely dependent on CSF-1 (Fig. 1, A and B; and Fig. 4 A; Davies et al., 2013). Treatment with IL-4c did not increase production of CSF-1 in either serum or tissues, consistent with an intrinsic and CSF-1–independent effect of IL-4 on MΦs. Thus, it would appear that IL-4Rα signaling to MΦs allows their substantial outgrowth above normal tissue levels at least in part by switching them to a CSF-1–independent program of proliferation.

Nevertheless, IL-4R$^+$ MΦs remain reliant on CSF-1 for survival after IL-4–driven expansion, as indicated by the reduced numbers observed after CSF1R blockade. Seemingly at odds with such a requirement, we found that IL-4 treatment was accompanied by a sharp down-regulation in MΦ transcription of the CSF1R. However, lower levels of CSF1R signaling are required for MΦ survival than are needed for their proliferation (Tushinski et al., 1982). CSF-1 is likely present in the steady-state serous cavities in greater abundance than required for MΦ survival given the evident homeostatic CSF-1–dependent proliferation in these sites (Figs. 1 and 4; Davies et al., 2013). We suggest that IL-4–mediated down-regulation of CSF1R reduces local CSF-1 consumption by individual cells, thereby maintaining sufficient tissue CSF-1 levels to allow survival of the expanding MΦ population. Such a model would explain how the basal levels of proliferation and total number of IL-4Rα$^-$ MΦs in mixed BM chimeras appeared to be maintained at near normal steady-state levels after treatment with IL-4c (Fig. 2 E) despite the large outgrowth of IL-4Rα$^+$ cells and without a corresponding increase in CSF-1 production (Fig. 1 D). Together, our data suggest that IL-4 and CSF-1 are entirely distinct in terms of proliferation although CSF-1 is still critical for survival in the context of IL-4 expansion.

During nematode infection, our data suggest that CSF-1 plays an early role in MΦ proliferation but is superseded by IL-4 presumably upon entry of Th2 cells. Supporting this, CSF1R blockade during infection almost completely inhibited proliferation in all WT animals except those exhibiting the highest levels of IL-4 exposure, as indicated by the percentage of cells expressing alternative activation markers (Fig. 4 A). Furthermore, time course analysis during infection demonstrated that proliferation occurred before, but only peaked after, the onset of alternative activation (Fig. 3 D), whereas more sustained and higher proliferation was achieved by IL-4Rα$^+$ than IL-4Rα$^-$ cells in infected mixed BM chimeric mice (Fig. 5 A). Lastly, the restriction of proliferation and MΦ accumulation to the infection site, and the absence of any such response in *Rag1*$^{-/-}$ animals (Fig. 5, E and F), mirrors our previous findings that MΦs fail to accumulate in a related nematode infection in the absence of Th2 cells (Loke et al., 2007). IL-4 may also contribute to elevated tissue MΦ density during infection through additional cell-intrinsic mechanisms, for example, by reducing reliance on local glucose levels (Vats et al., 2006), inhibiting migration from the tissue

positive for BrdU, Ki67, Ym1, and RELMα$^+$ was determined on day 7. Data are representative of three experiments with three to four mice per group. *, $P < 0.05$; **, $P < 0.01$; and ***, $P < 0.001$ determined by ANOVA. (C) As in B but after treatment of BALB/c mice with anti-CSF1R mAb (CSF1R) or rat IgG (IgG) on day 6. (D) *Il4ra*$^{+/+}$*Cd45.1*$^+$*Cd45.2*$^+$ mice were lethally irradiated and reconstituted for 8 wk with a 50:50 mix of *Il4ra*$^{+/+}$*Cd45.1*$^+$*Cd45.2*$^+$ and *Il4ra*$^{-/-}$*Cd45.1*^{null}*Cd45.2*$^+$ congenic BM cells before infection with *Hp*. The frequency of CD45.1$^+$ cells in different leukocyte subsets in the peritoneal cavity in naive (open symbols) and *Hp*-infected mice (closed symbols) was determined on days 7 and 14 after infection. The graphs show total numbers of *Il4ra*$^{+/+}$*Cd45.1*$^+$ and *Il4ra*$^{-/-}$*Cd45.1*^{null} peritoneal F4/80^{High} MΦs obtained in naive (open) and infected (closed) mice at each time point. (E) *Il4ra*$^{-/lox}$ (Het), *LysM*^{cre}*Il4ra*$^{-/lox}$ (Lys), or *Il4ra*$^{-/-}$ (−/−) mice were infected with *Hp*, and RELMα expression by F4/80^{High} peritoneal MΦs was determined on days 14 and 28. (C–E) Data are from independent experiments performed once and are confirmatory of data from the *Ls* model. (B–E) Horizontal bars indicate mean values.

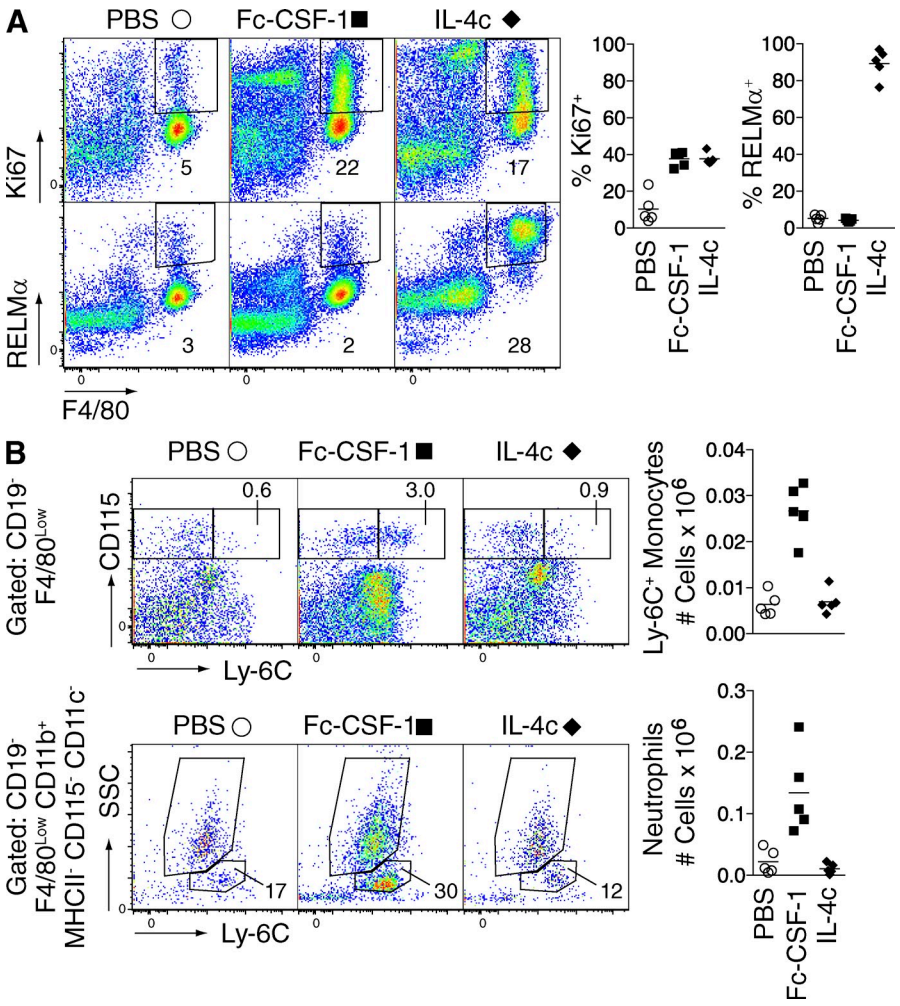

Figure 7. CSF-1 but not IL-4 stimulates neutrophil and monocyte recruitment alongside elevated proliferation of resident tissue MΦs. (A) BL/6 mice were injected i.p. with PBS, Fc-CSF-1, or IL-4c, and Ki67 and RELMα expression by F4/80^{High} peritoneal MΦs was determined 24 h later. Representative flow cytograms show all live peritoneal lavage cells. Data are representative of two independent experiments. (B) Total Ly-6C^{+}CD115^{+} monocytes and Ly-6C^{Intermediate}SSC^{Intermediate} neutrophils in peritoneal lavage cells from mice in A and representative flow cytograms depicting gating strategies. Top flow cytograms also depict CD115^{+}Ly6C^{-} monocytes/MΦs (left gate), and bottom flow cytograms show the SSC^{High}Ly6C^{Low} eosinophil gate, both of which exhibited no change in total number. (A and B) Horizontal bars indicate mean values.

(Thomas et al., 2012), or protecting against apoptosis, as occurs in other leukocytes (Wurster et al., 2002). Although the mixed *Il4ra*$^{+/+}$: *Il4ra*$^{-/-}$ BM mice do not reflect the natural distribution of IL-4R expression in vivo, they are critically important for understanding how cell-intrinsic IL-4R signaling augments MΦ numbers during nematode infection. Furthermore, the data generated using these mice may be relevant to circumstances in which differential IL-4R expression does occur (Wermeling et al., 2013).

RELMα and Ym1 were used here as surrogate markers of IL-4R–experienced MΦs. Elsewhere, Ym1 expression has been documented in MΦs from *LysM*^{cre}*Il4ra*$^{-/lox}$ mice in the liver granulomas surrounding schistosome eggs and peritoneal cavity after injection of schistosome eggs (Dewals et al., 2010). Because Ym1 expression is reduced significantly by in vivo IL-10 blockage, it was concluded that IL-10 induces MΦ Ym1 expression in these settings independently of IL-4 (Dewals et al., 2010). However, we observed a large proportion of serous cavity MΦs in *LysM*^{cre}*Il4ra*$^{-/lox}$ mice expressing Ym1 and RELMα in response to IL-4c injection and during infection with *Ls* or *Hp*, with costaining confirming IL-4Rα expression. Moreover, expression of both Ym1 and RELMα was exclusively restricted to IL-4Rα^{+} MΦs in IL-4–treated or nematode-infected mixed BM chimeric mice despite abundant IL-10 detectable in the pleural lavage fluid during infection (not depicted). It would seem that the selective advantage of IL-4Rα expression leads to accrual of a minor non-gene–deleted population, which could account for the Ym1^{+} cells observed in *LysM*^{cre}*Il4ra*$^{-/lox}$ mice during schistosome infection (Dewals et al., 2010). Alternatively, MΦs elicited by schistosome eggs may differ qualitatively from those found during nematode infection and IL-4c injection, being capable of Ym1 production in response to IL-10. In this respect, schistosome eggs elicit CCR2-dependent inflammatory MΦs (Chensue et al., 1996; Lu et al., 1998), contrasting with the resident-derived cells in our systems (Jenkins et al., 2011). Furthermore, *Il4ra*$^{-/-}$ and *LysM*^{cre}*Il4ra*$^{-/lox}$ mice show no defect in overall MΦ numbers elicited to schistosome granulomas (Dewals et al., 2010), perhaps because of the proinflammatory nature of the eggs. Therefore, the balance of proliferation versus recruitment in Th2 settings almost certainly depends on integration of multiple inflammatory signals. Of relevance, variation of IL-4c dose and delivery timing suggested that proliferation may only be apparent in environments in which critical IL-4 thresholds are sustained.

Steady-state proliferation in naive animals was not influenced by IL-4Rα signaling in mixed BM chimeric mice, *LysM*^{cre}*Il4ra*$^{-/lox}$ mice, or in global IL-4Rα–deficient animals, demonstrating that IL-4 mediates density of cavity MΦs only under conditions of inflammation and not homeostasis. IL-4Rα signaling also had little or no bearing on the wholly CSF-1–dependent elevated proliferation of resident peritoneal MΦs that occurs during resolution of microbial-induced peritonitis (Davies et al., 2013). In this process, however, proliferation acts simply to restore the MΦ population to its original level after depletion during the acute stage of inflammation (Davies et al., 2011) and is therefore akin to homeostatic maintenance rather than an inflammatory process. In keeping with this, the levels of CSF-1 did not differ between naive and inflammatory-challenged mice in this study (Davies et al., 2013). Elevated levels of circulating CSF-1 do occur in many disease states, and administration of CSF-1 can greatly increase tissue MΦ numbers in rodents and primates (Hume and MacDonald, 2012), but it is unclear whether this increase results from the outgrowth of resident MΦs or recruitment of new monocyte-derived cells. Using a recombinant Fc–CSF-1 fusion protein, we demonstrate that CSF-1 efficiently stimulates proliferation of resident peritoneal MΦs (Fig. 7 A). Furthermore, during nematode infection, we detected an approximate doubling in the number of IL-4Rα–deficient MΦs in mixed BM chimeras (Fig. 5 A) and in global *Il4ra*$^{-/-}$ mice (Fig. 3 B), mirroring the twofold increase in local CSF-1 production (Fig. 4 B). Elevated CSF-1 can therefore act during an inflammatory episode to increase local numbers of resident tissue MΦs and could play a more significant role in expansion of resident MΦs in pathologies in which much higher CSF-1 levels are observed (Hamilton, 2008).

Although both IL-4 and CSF-1 elicited proliferation of resident MΦs, they differed fundamentally in other actions. In particular, injection of Fc–CSF-1 also induced recruitment of Ly6C$^+$ monocytes and neutrophils, consistent with studies elsewhere (Lenda et al., 2003; Tagliani et al., 2011), suggesting elevated CSF-1 secretion may act as an emergency stopgap to rapidly fill the tissue MΦ compartment. In contrast, we saw no evidence of increased recruitment of inflammatory cells after IL-4c administration and previously observed recruitment of only low numbers during the early stages of *Ls* infection despite the large increase in resident tissue MΦs (Jenkins et al., 2011). CSF1R signaling directly induces production of CCR2 ligands by tissue MΦs to stimulate recruitment of Ly-6C$^+$ monocytes (Tagliani et al., 2011), whereas IL-4 down-regulates MΦ production of CCL2, CCL7, and CCL3 during tissue nematode infection (Thomas et al., 2012). Although the finding that IL-4–mediated proliferation is CSF1R independent was at first unexpected, our data suggest that this mechanism may have developed as an alternative to a CSF-1 pathway to increase numbers of resident MΦs without coincident increase in monocyte recruitment. This could be seen as an additional tissue-protective function of IL-4 beyond induction of the immunoregulatory and pro-wound repair phenotype associated with alternative activation (Murray and Wynn, 2011).

In summary, the impact of IL-4 during infections is likely twofold: it increases numbers without the need for recruitment, whereas in the presence of recruitment it insures a noninflammatory environment by switching MΦs to an alternatively activated phenotype. Thus, the numerical advantage provided by MΦ IL-4Rα expression combined with the anti-inflammatory chemokine profile and alternative activation state ultimately leads to the development of a noninflammatory environment to contain worm infection and repair tissue regardless of MΦ source.

MATERIALS AND METHODS

Mice. BALB/c *Il4*$^{-/-}$ (Noben-Trauth et al., 1996), *Il4ra*$^{-/-}$, *LysM*^{cre}*Il4ra*$^{-/lox}$, and *Il4ra*$^{-/lox}$ mice (Herbert et al., 2004), C57BL/6 *Il4ra*$^{-/-}$ and *Rag1*$^{-/-}$ mice, and WT controls were bred and maintained in specific pathogen–free facilities at the University of Edinburgh. All experiments were permitted under a Project License granted by the Home Office UK and were approved by the University of Edinburgh Ethical Review Process. Experimental mice were age and sex matched. C57BL/6 *Il4ra*$^{-/-}$ mice were generated by backcrossing from the BALB/c *Il4ra*$^{-/-}$ strain a minimum of nine times. Competitive mixed BM chimeric mice were created by lethally irradiating C57BL/6 *Cd45.1*$^+$*Cd45.2*$^+$ mice with 11.5 Gy γ radiation administered in two doses ∼3 h apart, followed by i.v. injection of with 5 × 10^6 BM cells depleted of mature T cells using CD90 microbeads (Miltenyi Biotec) and comprised of a 1:1 mix of cells from C57BL/6 *Cd45.2*$^{+/+}$*Il4ra*$^{-/-}$ mice and C57BL/6 *Cd45.1*$^+$*Cd45.2*$^+$ mice. Chimeric animals were left for at least 8 wk before further experimental manipulation.

Parasites and reagents. *Hp* and *Ls* life cycles were maintained, and infective third-stage larvae (L3) were obtained as described elsewhere (Behnke and Wakelin, 1977; Le Goff et al., 2002). Mice were infected with 200 *Hp* L3 by oral gavage or 25 *Ls* L3 by s.c. injection. IL-4–anti–IL-4 mAb complex (IL-4c) was prepared as described previously (Finkelman et al., 1993), and unless stated otherwise, mice were injected i.p. with 5 µg of recombinant IL-4 (13.5 kD; PeproTech) complexed to 25 µg 11B11 (Bio X Cell) or 100 µl PBS vehicle control on days 0 and 2, and peritoneal and pleural exudate cells were harvested on day 4. IL-13–anti–IL-13 complexes were similarly prepared using 5 µg of recombinant IL-13 (12.3 kD; PeproTech) complexed to 25 µg eBio13A (eBioscience). Fc–CSF-1 is a fusion protein of pig CSF-1 with the Fc region of pig IgG1A (43.82 kD total) that was produced using mammalian cell line expression by Zoetis for D. Hume (UK patent application GB1303537.1). CSF-1 was conjugated to Fc for increased stability in vivo. Extensive experiments in mice and pigs reveal that pig CSF-1 is equally active in mice (Gow et al., 2012). The presence of endotoxin-like activity in Fc–CSF-1 was tested in murine BM-derived MΦs. There was no detectable induction of the LPS-responsive TNF gene under conditions in which LPS induced the gene >1,000-fold. Mice were injected i.p. with 20 µg Fc–CSF-1 in PBS. Where specified, mice were given 1 mg BrdU i.p. 3 h before the experimental end point.

Isolation of cells from the peritoneal and pleural cavity. Mice were sacrificed by exsanguination via the brachial artery under terminal anesthesia. After sacrifice, pleural or peritoneal cavity exudate cells were obtained by washing of the cavity with lavage media comprised of RPMI 1640 containing 2 mM L-glutamine, 200 U/ml penicillin, 100 µg/ml streptomycin, and 2 mM EDTA (Invitrogen). The first 2 or 3 ml of lavage wash supernatant from the pleural or peritoneal cavities, respectively, was frozen before analysis by ELSIA. Worm burden in the pleural lavage fluid of *Ls*-infected mice was determined by counting under a stereomicroscope (MZ9; Leica). Erythrocytes were removed by incubating with red blood cell lysis buffer. Cellular content of the cavities and organs was assessed by cell counting using a Casy TT cell counter (Roche) in combination with multicolor flow cytometry.

Flow cytometry. Equal numbers of cells or 20 µl of blood was stained for each sample. Blood samples were mixed and washed with Hank's buffered

saline solution containing 2 mM EDTA (Invitrogen). Cells were stained with LIVE/DEAD (Invitrogen). All samples were then blocked with 5 µg/ml anti-CD16/32 (2.4G2; produced in-house) and heat-inactivated normal mouse serum (1:20) in FACS buffer (0.5% BSA and 2 mM EDTA in Dulbecco's PBS) before surface staining on ice with antibodies to F4/80 (BM8), Siglec-F (E50-2440), Ly-6C (AL-21 or HK1.4), Gr-1 (RB6-8C5), CD11b (M1/70), CD11c (N418), MHCII (M5/114.15.2), CD19 (eBio1D3), CD4 (GK1.5), CD3 (17A2), CD115 (AFS98), IL-4Rα (mIL4R-M1), CD45.1 (A20), or CD45.2 (104; eBioscience or BD). Erythrocytes in blood samples were lysed using FACS Lyse solution (BD).

Detection of intracellular RELMα, Ym1, Ki67, and BrdU was performed directly ex vivo. Cells were stained for surface markers then fixed and permeabilized using FoxP3 staining buffer set (eBioscience). For BrdU staining, cells were incubated first with or without DNase for 30 min at 37°C. Cells were then stained with biotinylated goat anti-Ym1 (R&D Systems), purified polyclonal rabbit anti-RELMα (PeproTech), or directly labeled mAbs to Ki67 (B57) or anti-BrdU (B44 or Bu20a; BD or BioLegend), followed by Zenon anti–rabbit reagent (Invitrogen) or streptavidin-conjugated fluorochromes (BioLegend). Expression of Ym1, RELMα, and Ki67 was determined relative to appropriate polyclonal or monoclonal isotype control, whereas incorporation of BrdU was determined relative to staining on non-DNase–treated cells. Analysis of proliferation and alternative activation was performed on single live cells, determined using LIVE/DEAD and forward scatter (FSC) width (FSC-W) versus FSC area (FSC-A), respectively, and subsequently gated on $CD19^-$ cells to remove B cell–MΦ doublets. Analysis for calculation of total $F4/80^{High}$ MΦs was performed on all cells. Samples were acquired using FACS LSRII or FACSCanto II using FACSDiva software (BD) and analyzed with FlowJo version 9 software (Tree Star).

Analysis of MΦs from competitive mixed BM chimeras. MΦs derived from *Cd45.1*$^+$*Il4ra*$^{+/+}$ BM appeared to have a greater tendency to form doublets with $CD19^+$ B cells after injection of IL-4c than cells derived from *Cd45.1*$^-$*Il4ra*$^{-/-}$ BM, as judged by the high level of F4/80 expression on B cell–MΦ doublets (Fig. S2 A), a marker which is known to be up-regulated by IL-4R signaling (Jenkins et al., 2011). If doublets were excluded from analysis, such bias in doublet formation would distort the ratio of WT to *Il4ra*$^{-/-}$ MΦs. Thus, cells were treated for 5 min with Accumax cell aggregate dissociation medium (eBioscience) immediately before fixation, and population frequency analysis was performed without a single cell gate applied. To further prevent bias induced by the few remaining doublets, the gate for $CD45.1^+$ $CD45.2^+$ cells was set to exclude events that deviated from the expected linear relationship of CD45.1 and CD45.2 on this population (Fig. S2 B, R1). Analysis of proliferation and alternative activation in these experiments was performed on $CD19^-F4/80^{High}$ MΦs gated on single cells, using FSC-W versus FSC-A, to minimize the potential for false positives (Fig. S2 B, R2). Because of a minor bias toward more WT than *Il4ra*$^{-/-}$ pleural MΦs in naive chimeras, one-way ANOVA was used to analyze differences in cell numbers after infection, whereas paired statistical tests were used to analyze rates of proliferation and alternative activation, to better account for the variation in overall level of proliferation between mice.

CSF1R experiments. Mice were injected i.p. with 0.5 mg anti-CSF1R mAb (clone AFS98), purified rat IgG control antibody, or PBS vehicle control either concurrent with IL-4c injections or on day 8 after *Ls* infection or day 6 after *Hp* infection. AFS98 mAb and purified rat IgG control were produced in-house from cultured hybridoma cells or from naive rat serum, respectively. The c-fms kinase inhibitor GW2580 (LC Laboratories; Conway et al., 2005) was suspended in 0.5% hydroxypropylmethylcellulose and 0.1% Tween 20 using a Teflon glass homogenizer. Diluent control or 160 mg/kg GW2580 was administered daily by oral gavage from 1 h before initial dose of IL-4c on day 0 to 5 h before mice were culled on day 3. Previous pharmacokinetic analysis has shown this daily dose regimen is as effective as twice daily administration of 80 mg/kg and maintains a serum concentration of the drug over 24 h above that estimated to achieve therapeutic effect (Priceman et al., 2010). Analysis of CSF-1 in brachial arterial blood and pleural lavage fluid was performed according to the manufacturer's instruction (PeproTech).

MΦ purification and gene expression. Gene expression analysis on MΦs from IL-4c– or PBS-treated mice was performed on mRNA for which we have previously published data (Rückerl et al., 2012). In brief, 24 h after treatment of mice with PBS or IL-4c, peritoneal MΦs were sorted using a FACSAria cell sorter (BD) according to their expression of $F4/80^+$, Siglec-F^-, $CD11b^+$, $CD11c^-$, $B220^-$, $CD3^-$ to purities >90%. Total RNA was then isolated using the miRNEasy kit (QIAGEN) according to the manufacturer's instructions, measured using a NanoDrop (Thermo Fisher Scientific), and converted to cDNA with BioScript reverse transcription (Bioline) and p(dT)15 primers (Roche). Expression levels were quantified using LightCycler 480 SYBR Green I Master (Roche), with measurements performed on a LightCycler 480 (Roche). Expression of *Csf1r* (5′-CGAGGGAGACTC-CAGCTACA-3′ and 5′-GACTGGAGAAGCCACTGTCC-3′) was normalized against *Gapdh* (5′-ATGACATCAAGAAGGTGGTG-3′ and 5′-CATACCAGGAAATGAGCTTG-3′).

Statistics. Data were log-transformed to achieve normal distribution and equal variance where required and then tested using one-way ANOVA or Student's *t* test. Where equal variance or normal distribution was not achieved, Kruskal Wallace or Spearman correlation was used. Paired Student's *t* test was used to determine differences between proliferation and alternative activation of $CD45.1^+$ and $CD45.1^-$ MΦs obtained from *Ls*-infected competitive mixed BM chimeric mice. Statistics were performed using Prism 5 (GraphPad Software). Each data point represents one animal.

Online supplemental material. Fig. S1 shows that MΦs in S phase express the highest levels of Ki67, such that gating on $Ki67^{High}$ cells provides an accurate estimate of their frequency and provides representative flow cytograms of Ki67, RELMα, and Ym1 staining on peritoneal and pleural MΦs at various times after IL-4c injection. Fig. S2 shows the gating strategy used to determine frequency of MΦ subsets from competitive mixed BM chimera experiments. Online supplemental material is available at http://www.jem.org/cgi/content/full/jem.20121999/DC1.

We thank A. Fulton, S. Afrough, S. McGarvie, and E. Slattery for technical assistance and Dr. P. Taylor for critical reading of the manuscript.

This work was funded by the Medical Research Council UK (G0600818 and MR/K01207X/1 to J.E. Allen), with additional support from the Welcome Trust (strategic award for Centre for Immunity, Infection, and Evolution; 082611/Z/07/Z, PhD studentship to G.D. Thomas and grants to R.M. Maizels). F. Brombacher is a South African Research Chair holder supported by the National Research Foundation (South Africa) and South African Medical Research Council. D.A. Hume was supported by an Institute Strategic Programme Grant to the Roslin Institute from the Biotechnology and Biological Sciences Research Council (project grant BB/H012559/1).

The Fc-CSF-1 reagent is the subject of UK patent application GB1303537.1. The authors have no additional conflicting financial interests.

Submitted: 5 September 2012
Accepted: 30 August 2013

REFERENCES

Ajami, B., J.L. Bennett, C. Krieger, W. Tetzlaff, and F.M. Rossi. 2007. Local self-renewal can sustain CNS microglia maintenance and function throughout adult life. *Nat. Neurosci.* 10:1538–1543. http://dx.doi.org/10.1038/nn2014

Ajami, B., J.L. Bennett, C. Krieger, K.M. McNagny, and F.M. Rossi. 2011. Infiltrating monocytes trigger EAE progression, but do not contribute to the resident microglia pool. *Nat. Neurosci.* 14:1142–1149. http://dx.doi.org/10.1038/nn.2887

Alikhan, M.A., C.V. Jones, T.M. Williams, A.G. Beckhouse, A.L. Fletcher, M.M. Kett, S. Sakkal, C.S. Samuel, R.G. Ramsay, J.A. Deane, et al. 2011. Colony-stimulating factor-1 promotes kidney growth and repair via alteration of macrophage responses. *Am. J. Pathol.* 179:1243–1256. http://dx.doi.org/10.1016/j.ajpath.2011.05.037

Aziz, A., E. Soucie, S. Sarrazin, and M.H. Sieweke. 2009. MafB/c-Maf deficiency enables self-renewal of differentiated functional macrophages. *Science.* 326:867–871. http://dx.doi.org/10.1126/science.1176056

Behnke, J.M., and D. Wakelin. 1977. *Nematospiroides dubius*: stimulation of acquired immunity in inbred strains of mice. *J. Helminthol.* 51:167–176. http://dx.doi.org/10.1017/S0022149X0000746X

Bunting, K.D., W.M. Yu, H.L. Bradley, E. Haviernikova, A.E. Kelly-Welch, A.D. Keegan, and C.K. Qu. 2004. Increased numbers of committed myeloid progenitors but not primitive hematopoietic stem/progenitors in mice lacking STAT6 expression. *J. Leukoc. Biol.* 76:484–490. http://dx.doi.org/10.1189/jlb.0903440

Chensue, S.W., K.S. Warmington, J.H. Ruth, P.S. Sanghi, P. Lincoln, and S.L. Kunkel. 1996. Role of monocyte chemoattractant protein-1 (MCP-1) in Th1 (mycobacterial) and Th2 (schistosomal) antigen-induced granuloma formation: relationship to local inflammation, Th cell expression, and IL-12 production. *J. Immunol.* 157:4602–4608.

Chitu, V., and E.R. Stanley. 2006. Colony-stimulating factor-1 in immunity and inflammation. *Curr. Opin. Immunol.* 18:39–48. http://dx.doi.org/10.1016/j.coi.2005.11.006

Chorro, L., A. Sarde, M. Li, K.J. Woollard, P. Chambon, B. Malissen, A. Kissenpfennig, J.B. Barbaroux, R. Groves, and F. Geissmann. 2009. Langerhans cell (LC) proliferation mediates neonatal development, homeostasis, and inflammation-associated expansion of the epidermal LC network. *J. Exp. Med.* 206:3089–3100. http://dx.doi.org/10.1084/jem.20091586

Conway, J.G., B. McDonald, J. Parham, B. Keith, D.W. Rusnak, E. Shaw, M. Jansen, P. Lin, A. Payne, R.M. Crosby, et al. 2005. Inhibition of colony-stimulating-factor-1 signaling in vivo with the orally bioavailable cFMS kinase inhibitor GW2580. *Proc. Natl. Acad. Sci. USA.* 102:16078–16083. http://dx.doi.org/10.1073/pnas.0502000102

Dai, X.M., G.R. Ryan, A.J. Hapel, M.G. Dominguez, R.G. Russell, S. Kapp, V. Sylvestre, and E.R. Stanley. 2002. Targeted disruption of the mouse colony-stimulating factor 1 receptor gene results in osteopetrosis, mononuclear phagocyte deficiency, increased primitive progenitor cell frequencies, and reproductive defects. *Blood.* 99:111–120. http://dx.doi.org/10.1182/blood.V99.1.111

Davies, L.C., M. Rosas, P.J. Smith, D.J. Fraser, S.A. Jones, and P.R. Taylor. 2011. A quantifiable proliferative burst of tissue macrophages restores homeostatic macrophage populations after acute inflammation. *Eur. J. Immunol.* 41:2155–2164. http://dx.doi.org/10.1002/eji.201141817

Davies, L.C., M. Rosas, S.J. Jenkins, C.T. Liao, M.J. Scurr, F. Brombacher, D.J. Fraser, J.E. Allen, S.A. Jones, and P.R. Taylor. 2013. Distinct bone marrow-derived and tissue-resident macrophage lineages proliferate at key stages during inflammation. *Nat. Commun.* 4:1886. http://dx.doi.org/10.1038/ncomms2877

DeNardo, D.G., J.B. Barreto, P. Andreu, L. Vasquez, D. Tawfik, N. Kolhatkar, and L.M. Coussens. 2009. CD4(+) T cells regulate pulmonary metastasis of mammary carcinomas by enhancing protumor properties of macrophages. *Cancer Cell.* 16:91–102. http://dx.doi.org/10.1016/j.ccr.2009.06.018

Dewals, B.G., R.G. Marillier, J.C. Hoving, M. Leeto, A. Schwegmann, and F. Brombacher. 2010. IL-4Ralpha-independent expression of mannose receptor and Ym1 by macrophages depends on their IL-10 responsiveness. *PLoS Negl. Trop. Dis.* 4:e689. http://dx.doi.org/10.1371/journal.pntd.0000689

Finkelman, F.D., K.B. Madden, S.C. Morris, J.M. Holmes, N. Boiani, I.M. Katona, and C.R. Maliszewski. 1993. Anti-cytokine antibodies as carrier proteins. Prolongation of in vivo effects of exogenous cytokines by injection of cytokine-anti-cytokine antibody complexes. *J. Immunol.* 151:1235–1244.

Fleetwood, A.J., T. Lawrence, J.A. Hamilton, and A.D. Cook. 2007. Granulocyte-macrophage colony-stimulating factor (CSF) and macrophage CSF-dependent macrophage phenotypes display differences in cytokine profiles and transcription factor activities: implications for CSF blockade in inflammation. *J. Immunol.* 178:5245–5252.

Gordon, S., and F.O. Martinez. 2010. Alternative activation of macrophages: mechanism and functions. *Immunity.* 32:593–604. http://dx.doi.org/10.1016/j.immuni.2010.05.007

Gow, D.J., V. Garceau, R. Kapetanovic, D.P. Sester, G.J. Fici, J.A. Shelly, T.L. Wilson, and D.A. Hume. 2012. Cloning and expression of porcine Colony Stimulating Factor-1 (CSF-1) and Colony Stimulating Factor-1 Receptor (CSF-1R) and analysis of the species specificity of stimulation by CSF-1 and Interleukin 34. *Cytokine.* 60:793–805. http://dx.doi.org/10.1016/j.cyto.2012.08.008

Hamilton, J.A. 2008. Colony-stimulating factors in inflammation and autoimmunity. *Nat. Rev. Immunol.* 8:533–544. http://dx.doi.org/10.1038/nri2356

Hashimoto, D., A. Chow, C. Noizat, P. Teo, M.B. Beasley, M. Leboeuf, C.D. Becker, P. See, J. Price, D. Lucas, et al. 2013. Tissue-resident macrophages self-maintain locally throughout adult life with minimal contribution from circulating monocytes. *Immunity.* 38:792–804. http://dx.doi.org/10.1016/j.immuni.2013.04.004

Heller, N.M., X. Qi, I.S. Junttila, K.A. Shirey, S.N. Vogel, W.E. Paul, and A.D. Keegan. 2008. Type I IL-4Rs selectively activate IRS-2 to induce target gene expression in macrophages. *Sci. Signal.* 1:ra17. http://dx.doi.org/10.1126/scisignal.1164795

Herbert, D.R., C. Hölscher, M. Mohrs, B. Arendse, A. Schwegmann, M. Radwanska, M. Leeto, R. Kirsch, P. Hall, H. Mossmann, et al. 2004. Alternative macrophage activation is essential for survival during schistosomiasis and downmodulates T helper 1 responses and immunopathology. *Immunity.* 20:623–635. http://dx.doi.org/10.1016/S1074-7613(04)00107-4

Hume, D.A. 2011. Applications of myeloid-specific promoters in transgenic mice support in vivo imaging and functional genomics but do not support the concept of distinct macrophage and dendritic cell lineages or roles in immunity. *J. Leukoc. Biol.* 89:525–538. http://dx.doi.org/10.1189/jlb.0810472

Hume, D.A., and K.P. MacDonald. 2012. Therapeutic applications of macrophage colony-stimulating factor-1 (CSF-1) and antagonists of CSF-1 receptor (CSF-1R) signaling. *Blood.* 119:1810–1820. http://dx.doi.org/10.1182/blood-2011-09-379214

Hume, D.A., P. Pavli, R.E. Donahue, and I.J. Fidler. 1988. The effect of human recombinant macrophage colony-stimulating factor (CSF-1) on the murine mononuclear phagocyte system in vivo. *J. Immunol.* 141:3405–3409.

Huynh, J., M.Q. Kwa, A.D. Cook, J.A. Hamilton, and G.M. Scholz. 2012. CSF-1 receptor signalling from endosomes mediates the sustained activation of Erk1/2 and Akt in macrophages. *Cell. Signal.* 24:1753–1761. http://dx.doi.org/10.1016/j.cellsig.2012.04.022

Irvine, K.M., C.J. Burns, A.F. Wilks, S. Su, D.A. Hume, and M.J. Sweet. 2006. A CSF-1 receptor kinase inhibitor targets effector functions and inhibits pro-inflammatory cytokine production from murine macrophage populations. *FASEB J.* 20:1921–1923. http://dx.doi.org/10.1096/fj.06-5848fje

Jenkins, S.J., and J.E. Allen. 2010. Similarity and diversity in macrophage activation by nematodes, trematodes, and cestodes. *J. Biomed. Biotechnol.* 2010:262609. http://dx.doi.org/10.1155/2010/262609

Jenkins, S.J., D. Ruckerl, P.C. Cook, L.H. Jones, F.D. Finkelman, N. van Rooijen, A.S. MacDonald, and J.E. Allen. 2011. Local macrophage proliferation, rather than recruitment from the blood, is a signature of TH2 inflammation. *Science.* 332:1284–1288. http://dx.doi.org/10.1126/science.1204351

Kanitakis, J., P. Petruzzo, and J.M. Dubernard. 2004. Turnover of epidermal Langerhans' cells. *N. Engl. J. Med.* 351:2661–2662. http://dx.doi.org/10.1056/NEJM200412163512523

Karp, C.L., and P.J. Murray. 2012. Non-canonical alternatives: What a macrophage is 4. *J. Exp. Med.* 209:427–431. http://dx.doi.org/10.1084/jem.20120295

Klein, I., J.C. Cornejo, N.K. Polakos, B. John, S.A. Wuensch, D.J. Topham, R.H. Pierce, and I.N. Crispe. 2007. Kupffer cell heterogeneity: functional properties of bone marrow derived and sessile hepatic macrophages. *Blood.* 110:4077–4085. http://dx.doi.org/10.1182/blood-2007-02-073841

Landberg, G., E.M. Tan, and G. Roos. 1990. Flow cytometric multiparameter analysis of proliferating cell nuclear antigen/cyclin and Ki-67 antigen: a new view of the cell cycle. *Exp. Cell Res.* 187:111–118. http://dx.doi.org/10.1016/0014-4827(90)90124-S

Le Goff, L., T.J. Lamb, A.L. Graham, Y. Harcus, and J.E. Allen. 2002. IL-4 is required to prevent filarial nematode development in resistant but not susceptible strains of mice. *Int. J. Parasitol.* 32:1277–1284. http://dx.doi.org/10.1016/S0020-7519(02)00125-X

Lenda, D.M., E. Kikawada, E.R. Stanley, and V.R. Kelley. 2003. Reduced macrophage recruitment, proliferation, and activation in

colony-stimulating factor-1-deficient mice results in decreased tubular apoptosis during renal inflammation. *J. Immunol.* 170:3254–3262.

Liao, X., N. Sharma, F. Kapadia, G. Zhou, Y. Lu, H. Hong, K. Paruchuri, G.H. Mahabeleshwar, E. Dalmas, N. Venteclef, et al. 2011. Krüppel-like factor 4 regulates macrophage polarization. *J. Clin. Invest.* 121:2736–2749. http://dx.doi.org/10.1172/JCI45444

Linde, N., W. Lederle, S. Depner, N. van Rooijen, C.M. Gutschalk, and M.M. Mueller. 2012. Vascular endothelial growth factor-induced skin carcinogenesis depends on recruitment and alternative activation of macrophages. *J. Pathol.* 227:17–28. http://dx.doi.org/10.1002/path.3989

Loke, P., I. Gallagher, M.G. Nair, X. Zang, F. Brombacher, M. Mohrs, J.P. Allison, and J.E. Allen. 2007. Alternative activation is an innate response to injury that requires CD4+ T cells to be sustained during chronic infection. *J. Immunol.* 179:3926–3936.

Lu, B., B.J. Rutledge, L. Gu, J. Fiorillo, N.W. Lukacs, S.L. Kunkel, R. North, C. Gerard, and B.J. Rollins. 1998. Abnormalities in monocyte recruitment and cytokine expression in monocyte chemoattractant protein 1-deficient mice. *J. Exp. Med.* 187:601–608. http://dx.doi.org/10.1084/jem.187.4.601

MacDonald, K.P., J.S. Palmer, S. Cronau, E. Seppanen, S. Olver, N.C. Raffelt, R. Kuns, A.R. Pettit, A. Clouston, B. Wainwright, et al. 2010. An antibody against the colony-stimulating factor 1 receptor depletes the resident subset of monocytes and tissue- and tumor-associated macrophages but does not inhibit inflammation. *Blood.* 116:3955–3963. http://dx.doi.org/10.1182/blood-2010-02-266296

Martinez, F.O., S. Gordon, M. Locati, and A. Mantovani. 2006. Transcriptional profiling of the human monocyte-to-macrophage differentiation and polarization: new molecules and patterns of gene expression. *J. Immunol.* 177:7303–7311.

Mohrs, K., D.P. Harris, F.E. Lund, and M. Mohrs. 2005. Systemic dissemination and persistence of Th2 and type 2 cells in response to infection with a strictly enteric nematode parasite. *J. Immunol.* 175:5306–5313.

Murphy, J., R. Summer, A.A. Wilson, D.N. Kotton, and A. Fine. 2008. The prolonged life-span of alveolar macrophages. *Am. J. Respir. Cell Mol. Biol.* 38:380–385. http://dx.doi.org/10.1165/rcmb.2007-0224RC

Murray, P.J., and T.A. Wynn. 2011. Protective and pathogenic functions of macrophage subsets. *Nat. Rev. Immunol.* 11:723–737. http://dx.doi.org/10.1038/nri3073

Nguyen, K.D., Y. Qiu, X. Cui, Y.P. Goh, J. Mwangi, T. David, L. Mukundan, F. Brombacher, R.M. Locksley, and A. Chawla. 2011. Alternatively activated macrophages produce catecholamines to sustain adaptive thermogenesis. *Nature.* 480:104–108. http://dx.doi.org/10.1038/nature10653

Noben-Trauth, N., G. Köhler, K. Bürki, and B. Ledermann. 1996. Efficient targeting of the IL-4 gene in a BALB/c embryonic stem cell line. *Transgenic Res.* 5:487–491. http://dx.doi.org/10.1007/BF01980214

Pello, O.M., M. De Pizzol, M. Mirolo, L. Soucek, L. Zammataro, A. Amabile, A. Doni, M. Nebuloni, L.B. Swigart, G.I. Evan, et al. 2012. Role of c-MYC in alternative activation of human macrophages and tumor-associated macrophage biology. *Blood.* 119:411–421. http://dx.doi.org/10.1182/blood-2011-02-339911

Priceman, S.J., J.L. Sung, Z. Shaposhnik, J.B. Burton, A.X. Torres-Collado, D.L. Moughon, M. Johnson, A.J. Lusis, D.A. Cohen, M.L. Iruela-Arispe, and L. Wu. 2010. Targeting distinct tumor-infiltrating myeloid cells by inhibiting CSF-1 receptor: combating tumor evasion of antiangiogenic therapy. *Blood.* 115:1461–1471. http://dx.doi.org/10.1182/blood-2009-08-237412

Rückerl, D., S.J. Jenkins, N.N. Laqtom, I.J. Gallagher, T.E. Sutherland, S. Duncan, A.H. Buck, and J.E. Allen. 2012. Induction of IL-4Rα-dependent microRNAs identifies PI3K/Akt signaling as essential for IL-4-driven murine macrophage proliferation in vivo. *Blood.* 120:2307–2316. http://dx.doi.org/10.1182/blood-2012-02-408252

Schulz, C., E. Gomez Perdiguero, L. Chorro, H. Szabo-Rogers, N. Cagnard, K. Kierdorf, M. Prinz, B. Wu, S.E. Jacobsen, J.W. Pollard, et al. 2012. A lineage of myeloid cells independent of Myb and hematopoietic stem cells. *Science.* 336:86–90. http://dx.doi.org/10.1126/science.1219179

Smith, J.L., A.E. Schaffner, J.K. Hofmeister, M. Hartman, G. Wei, D. Forsthoefel, D.A. Hume, and M.C. Ostrowski. 2000. ets-2 is a target for an akt (Protein kinase B)/jun N-terminal kinase signaling pathway in macrophages of motheaten-viable mutant mice. *Mol. Cell. Biol.* 20:8026–8034. http://dx.doi.org/10.1128/MCB.20.21.8026-8034.2000

Tagliani, E., C. Shi, P. Nancy, C.S. Tay, E.G. Pamer, and A. Erlebacher. 2011. Coordinate regulation of tissue macrophage and dendritic cell population dynamics by CSF-1. *J. Exp. Med.* 208:1901–1916. http://dx.doi.org/10.1084/jem.20110866

Thomas, G.D., D. Rückerl, B.H. Maskrey, P.D. Whitfield, M.L. Blaxter, and J.E. Allen. 2012. The biology of nematode- and IL4Rα-dependent murine macrophage polarization in vivo as defined by RNA-Seq and targeted lipidomics. *Blood.* 120:e93–e104. http://dx.doi.org/10.1182/blood-2012-07-442640

Tushinski, R.J., I.T. Oliver, L.J. Guilbert, P.W. Tynan, J.R. Warner, and E.R. Stanley. 1982. Survival of mononuclear phagocytes depends on a lineage-specific growth factor that the differentiated cells selectively destroy. *Cell.* 28:71–81. http://dx.doi.org/10.1016/0092-8674(82)90376-2

Ulich, T.R., J. del Castillo, L.R. Watson, S.M. Yin, and M.B. Garnick. 1990. In vivo hematologic effects of recombinant human macrophage colony-stimulating factor. *Blood.* 75:846–850.

Vats, D., L. Mukundan, J.I. Odegaard, L. Zhang, K.L. Smith, C.R. Morel, R.A. Wagner, D.R. Greaves, P.J. Murray, and A. Chawla. 2006. Oxidative metabolism and PGC-1beta attenuate macrophage-mediated inflammation. *Cell Metab.* 4:13–24. (published erratum appears in *Cell Metab.* 2006. 4:255) http://dx.doi.org/10.1016/j.cmet.2006.05.011

Verreck, F.A., T. de Boer, D.M. Langenberg, M.A. Hoeve, M. Kramer, E. Vaisberg, R. Kastelein, A. Kolk, R. de Waal-Malefyt, and T.H. Ottenhoff. 2004. Human IL-23-producing type 1 macrophages promote but IL-10-producing type 2 macrophages subvert immunity to (myco)bacteria. *Proc. Natl. Acad. Sci. USA.* 101:4560–4565. http://dx.doi.org/10.1073/pnas.0400983101

Volkman, A., N.C. Chang, P.H. Strausbauch, and P.S. Morahan. 1983. Differential effects of chronic monocyte depletion on macrophage populations. *Lab. Invest.* 49:291–298.

Wermeling, F., R.M. Anthony, F. Brombacher, and J.V. Ravetch. 2013. Acute inflammation primes myeloid effector cells for anti-inflammatory STAT6 signaling. *Proc. Natl. Acad. Sci. USA.* 110:13487–13491. http://dx.doi.org/10.1073/pnas.1312525110

Wu, D., A.B. Molofsky, H.E. Liang, R.R. Ricardo-Gonzalez, H.A. Jouihan, J.K. Bando, A. Chawla, and R.M. Locksley. 2011. Eosinophils sustain adipose alternatively activated macrophages associated with glucose homeostasis. *Science.* 332:243–247. http://dx.doi.org/10.1126/science.1201475

Wurster, A.L., V.L. Rodgers, M.F. White, T.L. Rothstein, and M.J. Grusby. 2002. Interleukin-4-mediated protection of primary B cells from apoptosis through Stat6-dependent up-regulation of Bcl-xL. *J. Biol. Chem.* 277:27169–27175. http://dx.doi.org/10.1074/jbc.M201207200

Yona, S., K.W. Kim, Y. Wolf, A. Mildner, D. Varol, M. Breker, D. Strauss-Ayali, S. Viukov, M. Guilliams, A. Misharin, et al. 2013. Fate mapping reveals origins and dynamics of monocytes and tissue macrophages under homeostasis. *Immunity.* 38:79–91. http://dx.doi.org/10.1016/j.immuni.2012.12.001